Elsevier Editorial System(tm) for Biochemical Engineering Journal
Manuscript Draft

Manuscript Number:

Title: Kinetic model of photoautotrophic growth of Chlorella sp microalga, isolated from the Setúbal lagoon.

Article Type: Full Length Article

Section/Category: Bioreactor Systems

Keywords: Microalgae
Photobioreactor
Monte Carlo
Growth Kinetics
Kinetic Parameters
Scale-up

Corresponding Author: Dr. Horacio Antonio Irazoqui, Ph.D.

Corresponding Author's Institution: INTEC (UNL-CONICET)

First Author: Josué M Heinrich, Doctor

Order of Authors: Josué M Heinrich, Doctor; Horacio Antonio Irazoqui, Ph.D.

Abstract: In this work a kinetic expression relating light availability in the culture medium with the rate of microalgal growth is obtained. This expression, which is valid for low illumination conditions, was derived from the reactions that take part in the light-dependent stage of photosynthesis. The kinetic expression obtained is a function of the biomass concentration in the culture, as well as of the local volumetric rate of absorption of photons, and only includes two adjustable parameters. In order to determine the value of these parameters and to test the validity of the hypotheses made, autotrophic cultures of the Chlorella sp. strain were carried out in a modified BBM medium at three CO2 concentrations in the gas stream, namely 0.034%, 0.34% and 3.4%. Moreover, the local volumetric rate of photon absorption was predicted based on a physical model of the interaction of the radiant energy with the suspended biomass, together with a Monte Carlo simulation algorithm. The proposed intrinsic expression of the biomass growth rate, together with the Monte Carlo radiation field simulator, are key to scale up photobioreactors when operating under low irradiation conditions, independently of the configuration of the reactor and of its light source.

Submitted manuscript:

Kinetic model of photoautotrophic growth of Chlorella sp microalga, isolated from the Setúbal lagoon.

Authors:

Heinrich Josué Miguel[1,2] and Irazoqui Horacio Antonio[1,2.*]

[1]- Group of Innovation on Bio-processes Engineering, Institute for the Technological Development of the Chemical Industry (INTEC), National Council of Scientific and Technological Research (CONICET) and University of Litoral (UNL), Santa Fe, Argentina

[2]- Group of Innovation on Bio-processes Engineering, Department of Biochemistry and Biological Sciences (FBCB), University of Litoral (UNL), Santa Fe, Argentina

*Corresponding author. Tel.:+054 342 4575215/ internal 172. Postal address: Grand Bourg 3677 (CP: S3002GSC), Santa Fe, Argentina. E-mail address: hirazo@santafe-conicet.gov.ar

Covering Letter:

In a broad sense, we may say that the light energy available for algal growth can be thought of as a substrate and consequently, the local volumetric rate of photon absorption is the key property of the radiant field to be included in growth rate expressions of photosynthetic microorganisms. In the submitted manuscript, the local volumetric rate of photon absorption in the culture medium clearly arises as being the property which links the radiant energy field with the algal growth kinetics through the initial photon capture step of the photosynthetic mechanism.

The design, control and optimization of photo-bioreactors call for intrinsic growth kinetic expressions, depending only on the intensive physicochemical properties of the culture medium and independent of the configuration and size of the experimental device used for

its determination, as well as of the features of the radiant energy source. The use of average values of the properties of the radiant field in growth kinetic expressions leads to systematic error in the choice or in the derivation of the growth kinetics and in the parameter assessment as it also happens in other related applications (Alfano, Irazoqui, Cassano). A growth kinetics that depends on the configuration and the size of the experimental photo-bioreactor, or in the characteristics of its light source, severely hampers the possibility of a rational change of scale and of the geometrical characteristics of the reactor as well as of the features of the light source.

Algal growth rates strongly depend on the rate of photon absorption by the photosynthetic systems of the algal cells per unit culture volume. Therefore, intrinsic growth kinetic models should be expressed as functions of the local volumetric rate of photon absorption. The objective of this work is the derivation of an intrinsic kinetic expression for the algal growth rate based on a simplified proposed pathway, explicitly showing its dependence on the light availability at every position in the culture, as well as on the biomass. The kinetic expression obtained depends on the local volumetric rate of absorption of photons with wavelengths in the visible range, r_{Vis}^{abs}, resulting as a consequence, sensitive to the existence of differently illuminated areas within the reactor. This kinetic expression is a physicochemical property, so that it functionally depends on other physicochemical variables and the expression is independent of the configuration of the reactor and the light source, allowing its use in scale-up processes.

We confirm that all elements of the submission are in compliance with the journal publishing ethics policy.

***Highlights (for review)**

In this work a kinetic expression is derived from the photosynthesis mechanism.

The expression consider the biomass concentration and the photon absorption rate

The kinetic parameters are computed considering the stratification inside the reactor

The kinetic is independent of the reactor configuration and of its light source.

TITLE.

Kinetic model of photoautotrophic growth of Chlorella sp microalga, isolated from the Setúbal lagoon.

AUTHOR NAMES AND AFFILIATIONS

Heinrich Josué Miguel[1,2] and Irazoqui Horacio Antonio[1,2,*]

[1]- Group of Innovation on Bio-processes Engineering, Institute for the Technological Development of the Chemical Industry (INTEC), National Council of Scientific and Technological Research (CONICET) and University of Litoral (UNL), Santa Fe, Argentina

[2]- Group of Innovation on Bio-processes Engineering, Department of Biochemistry and Biological Sciences (FBCB), University of Litoral (UNL), Santa Fe, Argentina

*Corresponding author. Tel.:+054 342 4575215/ internal 172. Postal address: Grand Bourg 3677 (CP: S3002GSC), Santa Fe, Argentina. E-mail address: hirazo@santafe-conicet.gov.ar

ABSTACT.

In this work a kinetic expression relating light availability in the culture medium with the rate of microalgal growth is obtained. This expression, which is valid for low illumination conditions, was derived from the reactions that take part in the light-dependent stage of photosynthesis. The kinetic expression obtained is a function of the biomass concentration in the culture, as well as of the local volumetric rate of absorption of photons, and only includes two adjustable parameters. In order to determine the value of these parameters and to test the validity of the hypotheses made, autotrophic cultures of the *Chlorella* sp. strain were carried out in a modified BBM medium at three CO_2 concentrations in the gas stream, namely 0.034%, 0.34% and 3.4%. Moreover, the local volumetric rate of photon absorption was predicted based on a physical model of the interaction of the radiant energy with the suspended biomass, together with a Monte Carlo simulation algorithm. The proposed intrinsic expression of the biomass growth rate, together with the Monte Carlo radiation field simulator, are key to scale up photobioreactors when operating under low irradiation conditions, independently of the configuration of the reactor and of its light source.

NOTATIONS

PBR	Photo-bioreactor
REF	Radiant EnergyField
VIS	Refers to the visible region of the spectrum: $400 < \lambda < 700nm$
t	Time [*day*]
x	Biomass concentration [$gr\ L^{-1}$]
r_x	Rate of biomass growth [$gr\ L^{-1}\ día^{-1}$]
λ	Radiation wavelength [*nm*]
$\alpha_\lambda(t)$	Spectral ligth absorption coefficient [cm^{-1}]
$\xi_\lambda(t)$	Spectral ligth scattering coefficient [cm^{-1}]
$B(\underline{\Omega}' \cdot \underline{\Omega})$	Ligth scattering phase function [*dimensionless*]
$r_\lambda^{abs}(\underline{r},t)$	spectraldistributionoflocalvolumetricrateof absorption of photons [$\mu mol\ ofphotonsmL^{-1}\ s^{-1}\ nm^{-1}$]
$r_{Vis}^{abs}(\underline{r},t)$	localvolumetricrateof absorption of photons-VIS, with $400 < \lambda < 700nm$ [$\mu mol\ photonsmL^{-1}\ s^{-1}$]
$\overline{r}_{Vis}^{abs}(t)$	averagevolumetricrateof absorption of photons-VIS, with $400 < \lambda < 700nm$ [$\mu mol\ photonsmL^{-1}\ s^{-1}$]
$g(r_{Vis}^{abs},t)$	distributionfunctionof reactor volumen fractionsamongall posible averagevolumetricrateof absorption of photons-VIS, r_{Vis}^{abs} [$(\mu mol\ photons)^{-1}mLs$]

1 - . INTRODUCTION

The use of microalgae as a source of oil for the production of biofuels has received much attention in recent years [1, 2]. This is mainly because these have minimal nutritional requirements and are able to use solar energy more efficiently than superior plants, including traditional crops such as wheat, corn, soybean, sugar cane, etc [3, 4]. They are not only able to grow at high rates thus rendering high yields of oil in terms of tons per hectare per year, but they can do so in contaminated sewage and sea waters, unfit for human consumption or agricultural use. It is also possible to carry out cultivation in arid zones, flood plains or lands not fit for agriculture, so algal culturing does not compete for land with traditional agriculture [5, 6]. Furthermore, not only the biodiesel industry paid attention to these microorganisms, but they have also been identified as a feedstock in the production of food and animal feed; as in environmental remediation agents for effluent treatment; as a source of high valued products for the food industry and cosmetics (such as pigments, antioxidants, PUFAs); and as a biotechnology platform for recombinant protein expression; etc. [7, 8, 9].

In the last decade there have been significant developments regarding each of the stages involved in the algal production process, considering both up-stream and down-stream operations. However, despite the significant progress made so far, there still remains the need of further research to achieve sustainable and economically viable technologies [10, 11, 12]. In the case of the culturing step, for example, it is necessary to solve issues such as (i) how to achieve an efficient illumination of the algal suspension; (ii) how to feed carbon dioxide to the culture, enabling the enrichment of the air stream with additional CO_2 while minimizing losses to the atmosphere; (iii) how to remove the oxygen produced during photosynthesis, which could inhibit cell growth, and; (iv) how the scaling must be performed from the laboratory culture reactor to the production scale reactor [13].

Autotrophic algae utilize water as an electron source; sunlight as a source of energy and carbon dioxide as a carbon source [14]. The light from a radiation source (either natural or artificial) reaches the crop through one or more transparent reactor boundaries. Within the culture, the energy carried by the light beams is partially absorbed by the suspended cells as rays reach deeper zones in the culture [10]. This phenomenon dependens on the light wavelength: the extent to which the absorption of radiant energy occurs is not the same irrespective of itswavelength, but presents a profile defined by two spectral zones of high absorption (from 400 to 500nm, and from 600 to 690nm), separated by a low absorption region (Fig. 1) ([15, 16]. Furthermore, algal cells suspended in the culture also cause elastic scattering of the light beams, so that part of the energy they carry is deflected from their direction previous to the encounter into new ones without energy loss [15]. The presence of absorption and elastic scattering of

radiation has two consequences:(i) within the reactor occur areas illuminated with varying degrees; and (ii) the spectral composition of light in deeper areas is different than the emission profile of the lamp, because the maximum of the light distribution progressively shifts toward wavelengths less useful for photosynthesis.

<Figure 1>

Figure 1. (□) absorption coefficient α_λ vs wavelength; and (×) scattering coefficient ξ_λ vs wavelength within the 400‑700 nm region for a 1.65 g L^{-1} *Chlorella* sp. suspension. (Adapted from Heinrich J. M. *et al*, 2012 [17])

The light available at a given position in the suspension depends on (i) the reactor and energy source layout; (ii) the emission power of the lamp and its spectral composition; (iii) the absorption and scattering of radiant energy by the cells in the crop; (iv) the reflection and refraction of energy beams at the reactor surfaces; and, (v) dispersion of energy due to the presence of bubbles or other particles in the culture medium, if they are present.

In a previous work [17, 18] a model of well mixed algal suspensions, considering them as a continuum with absorption and scattering centers homogeneously dispersed, was proposed. Given the temperatures involved in algal crops, light could be assimilated as a gas of photons which move in different directions with the speed of light. Based on this physical model, Monte Carlo algorithms were developed and computationally implemented with different purposes: one for the determination of optical properties of the suspensions of microalgae (including the spectral absorption coefficient of radiant energy α_λ, the spectral coefficients of radiant energy dispersion ξ_λ; and the phase function $B\left(\underline{\Omega}'\cdot\underline{\Omega}\right)$, associated with the scattering of radiant energy by suspended cells; and the other for the simulation of the field of radiant energy in PBRs [15-18]. With the obtained optical parameters, the simulation methodology was used to predict the REF in the PBR used in this work (Fig. 2). As a result it was possible to predict the value of the local volumetric rate of absorption of photons r_{Vis}^{abs} and its change with the algal culture growth. It was also possible to predict the changing degree of stratification of light in the reactor, through the computed distribution of reactor volumes $g\left(r_{Vis}^{abs},t\right)$ among the different values of the

volumetric rate of absorption of photons r_{Vis}^{abs}, resulting from the stratification of light. The results show how increasing microalgae concentration results in the presence of dark areas due to the self-shading effect, and how the spectral distribution of the light changes as the energy beams reach deeper areas in the culture.

The objective of this work is the derivation of an intrinsic kinetic expression for the algal growth rate based on a simplified proposed pathway, explicitly showing its dependence on the light availability at every position in the culture, as well as on the biomass concentration. For this it is necessary to single out, among the properties of the radiant energy field, that on which the algal growth rate is functionally dependent, and physical reasons why and how this dependence is expressed mathematically, besides proposing a methodology for the evaluation of this property at any position within the suspension. Consistently with the experimental runs, the kinetic expression was derived assuming low lighting conditions, thus precluding the posibility of photoinhibition. The choice of light as the controlling substrate is consistent with the usual practice in reactor analysis to determine the relative impact of each one of the ongoing processes (in this case, light absorption); and the property and the mathematical form through which it participates in the expression sought for the algal growth rate.

The kinetic expression obtained depends on the local volumetric rate of absorption of photons with wavelengths in the visible range, r_{Vis}^{abs}, resulting as a consequence, sensitive to the existance of differently illuminated areas within the reactor. This kinetic expression is a physicochemical property, so that it functionally depends on other physicochemical variables and the expression is independent of the configuration of the reactor and the light source, allowing its use in scale-up processes.

2. - MATERIALS AND METHODS

Microalgae and inoculum: A Chlorella sp microalga strain, isolated from the Setúbal Lagoon (Santa Fe, Argentina) kindly provided by Dr. AM Gagneten, FHUC, University of Litoral, was used in this work. Inocula were prepared as follows: Erlenmeyer flasks containing 750 ml of BBM medium [19] were sterilized for 15 minutes in autoclave at 121 ^{o}C, cooled and seeded with the microalgalstrain. Inocula were grown axenically at room temperature, lit by a daylight fluorescent lamp (16 W input power Philips lamp, Philips Argentina S A, Buenos Aires, Argentina). A stream of atmospheric air is sterilized by filtration (0.45 m pore filter). Then is bubbled through the suspension with the purpose of supplying

the inoculum with the CO_2 needed for growth, while the O_2 produced is removed. As they raise, the bubbles cause small swirls that keep the suspension well mixed. This process is discontinued when a sufficiently high concentration of cells (about 500 mg L^{-1}) is reached.

<Figure 2>

Figure 2: Photobioreactor [15]. It consists of a cylindrical annulus between two glass tubes, coaxiallyaligned to a daylight fluorescent lamp. Lamp diameter: 26mm; PBR internal diameter: 50mm; PBR external diameter: 250 mm; PBR height: 310mm. Headof culture media: 210mm.

<Table I>

Reactor and culture conditions: The PBR (Fig. 2) consists of two glass tubes 50 and 250mm outer diameter, respectively, coaxially aligned to a fluorescent daylight cylindrical lamp (Philips; diameter: 26 mm; power input:16W). In order to record the pH and to control the temperature of the culture as well as the air flow and the concentration of CO_2 in the gas stream, the reactor was connected to a cultivation platform LabFors3 (InforsHT). Microalgal cultures were carried out at three different conditions resulting from varying the concentration of carbon dioxide in the gas stream. In each experimental run, 500 ml of inoculum were used to start the culture in a 10 L PBR, already charged with 9.5 L of medium. The BBM culture medium was modified as shown in Table I in order to ensure that the pH and the osmotic pressure of the medium remain unaltered when the carbon dioxide concentration in the gas phase is changed. Also, the nitrate source of nitrogen in the original formulation was substituted by urea, in order to prevent changes in the pH of the culture caused by the metabolism of nitrate.

Simulation of the radiation field: The Monte Carlo method was employed to simulate the radiation field in the PBR. The procedure starts from the emission source. The emission of light by the lamp is superficial and isotropic (i.e. the intensity of the emitted light is independent of the direction of emission from any point on the lamp surface). Moreover, it is assumed that the lamp emits homogeneously throughout its entire surface. First, a position on the lamp surface is randomly chosen, and both a direction and a wavelength are assigned to each emitted photon according to the emission characteristics

of the radiation source. Successively, the trajectory of each photon among a sufficiently large number of them is simulated as they travel through the suspension until it reaches its eventual termination. Photons can be removed from the radiation field when they are absorbed by the microalgae suspension; when they impact on any opaque surface; or because they leave the reactor through the external glass wall. The reflection on the glass walls was modeled as that occurring on an interface without thickness. The reflection of photons on the reactor bottom and on its lid (both made on mirror-polished steel) were modeled as specular reflections. The effects of the probes and control devices (pHmeter, O_2 sensor, cold finger, temperature sensor, sampling port, etc.) on the radiation field were neglected. One by one, photons are emitted from the lamp in a succession, and in their way they undergo different events. Although the photons are emitted sequentially, it is important to keep in mind that all of them are simultaneous, and altogether simulate the radiation field distribution inside the reactor at every moment. This radiation field adjusts itself without delay to the evolution with time of the microalgae culture, following its changes in a permanent steady state [15].

Concentration of biomass: the biomass concentration was determined by the method of Total Suspended Solids [20]. For this, the cells contained in a 50mL aliquot of the culture medium were retained by a glass fiber filter (0.45 μm), washed with distilled water to remove residual medium and oven dried at 100 ^{o}C for 1 hour. The cell biomass was reported in grams of dry biomass per liter of culture medium [gDW L^{-1}].

Concentration of Chlorophylls: the content of total chlorophylls was determined using the technique reported by Ritchie [21]. For this, the cells in an aliquot of the culture medium were centrifuged, resuspended in distilled water and centrifuged again to remove traces of culture medium. Chlorophylls were extracted with ethyl alcohol at room temperature for 24 hours. The chlorophylls content was calculated from the absorbance at 632, 649 and 665nm, using the absorption coefficients reported in the same work.

Concentration of urea: determinationsof urea concentrationwere performed using a commercial enzyme kit Color2R Urea, from Wiener Lab.

3. - RESULTS AND DISCUSSION.

3.1 A kinetic model of cell growth.

A kinetic model of autotrophic growth of microalgae under low illumination conditions is derived, based on the simplified reaction pathway for the light-dependent stage of photosynthesis listed in Table II [22-24]. The simplified pathway proposed for the light-dependent stage starts with the absorption of radiant energy by photosystem II (PSII). In the antenna complex of PSII, radiant energy is captured by chlorophyll pigments. The speed of this "reaction" step equals the product of the rate of absorption of photons in the PSII, multiplied by an efficiency Φ_{II}. Since the absorption of photons occurs almost exclusively in PSII and PSI, the rate of absorption of photons in the PSII can be written as a fraction θ_{II} of the rate of absorption of photons per cell R_{VIS}^{abs}.

<Table II>

Then, the absorbed energy is carried to the reaction center of the photosystem, where a charge separation occurs at the specific pair of chlorophylls, giving rise to a hole h_{II}^{+} bearing a positive charge and an electron e_{II}^{-} Eq. (1). The hole-electron pair may recombine releasing termal energy Eq. (2). To prevent this to happen, each highly oxidative hole h_{II}^{+} is combined with an electron provided by an enzyme complex CE_{Mn} attached to PSII, which consists in a cluster of manganese atoms with different oxidation states. This cluster releases in a succesion four electronsto the PSII complex Eqs. (3.1) to (3.4) thus neutralizing four positively charged holes. The four electrons are replenished at once by oxidation of two molecules of water to produce oxygen and protons Eq. (3.5), thus returning the the cluster to its initial oxidation state.

The electron e_{II}^{-}, which was the partner of the annihilated hole h_{II}^{+} is used to reduce a quinone Q, temporarily attached to PSII. This quinone is capable of accepting two electrons producing hydroquinone QH_2 Eq. (4.1) and (4.2). Thereafter the hydroquinone is oxidized in the cytochrome *b6/f* Eq. (5.1) coupled with the sequential reduction of two plastocyanin molecules PC Eqs. (5.2) and (5.3). Furthermore, in the cytochrome *b6/f*, a reaction known as *Q-cycle* is produced. When the reaction follows this way, the quinone Q produced in reaction 5.1 is further reduced to recover hydroquinone QH_2; the net result is the transport of two protons. Then, absorption of another photon in the PSI occurs.

The process of absorption and charge separation takes place in a manner analogous to what occurred in the PSII, except that in this case a plastocyanin molecule is the donor of electrons to neutralize the positivelycharged hole h_I^+; and ferredoxin $Ferr$ is the final electron acceptor.

The simplified pathway proposed for the light-dependent stage starts with the absorption of radiant energy by photosystem II (PSII). The light-dependent stage is followed by a network of enzymatic reactions not directly related to the use of radiant energy, but its main substrates are the products of the light dependent mechanisms that occur in the PSII and PSI. One of these reactions uses two molecules of ferredoxin to produce NADPH from $NADP^+$ Eq. (10); and another involves the use of potential energy stored as a proton gradient to catalyze formation of ATP from ADP and P_i Eq. (11). Both ATP and NADPH are substrates for many enzymatic reactions. Among them is the CO_2 fixation reaction by RubisCO enzyme [23,24].

$$2Ferr^- + NADP^+ + H_{ext}^+ \xrightarrow{Ferr-NADP\ \ Reductase} 2Ferr + NADPH \quad (10)$$

$$ADP + P_i + H_{int}^+ \xrightarrow{ATP\ \ Sintase} ATP + H_{ext}^+ \quad (11)$$

Given that our operating conditions are such that the absorption of radiant energy is the rate limiting step for cell growth, we will make the following assumptions:

• The energy harvesting stage is the limiting step of growth, and the rate of cell growth is proportional to the intracellular rate of formation of $Ferr^-$ Eq. (9).

• All the intermediate compounds involved in the electron transport reactions are at their kinetic steady state. There is no accumulation of such species within the cells, so that their intracellular rate of formation equals that of their consumption.

• Total intracellular concentrations of the compounds, enzymes and cellular structural materials involved in the transport of electrons are approximately constant during growth.

• The ratio of the concentration of the oxidized form to that of the reduced form of each compound is constant.

With the assumption of kinetic steady state of short lived intermediates, we have:

$$r_{h_I^+} = 0 = r_6 - r_7 - r_8 \quad (12)$$

$$r_{h_I^+} = 0 = \Phi_I \left(1-\theta_{II}\right) R_{VIS}^{abs} - k_7 \left[e_I^-\right]\left[h_I^+\right] - k_8 \left[h_I^+\right]\left[PC^-\right] \tag{13}$$

$$r_{e_I^-} = 0 = r_6 - r_7 - r_9 \tag{14}$$

$$r_{e_I^-} = 0 = \Phi_I \left(1-\theta_{II}\right) R_{VIS}^{abs} - k_7 \left[e_I^-\right]\left[h_I^+\right] - k_9 \left[e_I^-\right]\left[Ferr\right] \tag{15}$$

From Eqs. (13) and (15):

$$\left[e_I^-\right] = \frac{k_9 \left[Ferr\right]}{2k_7}\left(\sqrt{1+\frac{4\Phi_I \left(1-\theta_{II}\right) R_{VIS}^{abs} k_7}{k_8 k_9 \left[PC^-\right]\left[Ferr\right]}} - 1\right) \tag{16}$$

$$\left[h_I^-\right] = \frac{k_8 \left[PC^-\right]}{2k_7}\left(\sqrt{1+\frac{4\Phi_I \left(1-\theta_{II}\right) R_{VIS}^{abs} k_7}{k_8 k_9 \left[PC^-\right]\left[Ferr\right]}} - 1\right) \tag{17}$$

Considering the assumption regarding the proportionality of rate of cell growth with the intracellular rate of formation of $Ferr^-$, we may write:

$$r_x = K_1 r_9 = K_1 k_9 \left[e_I^-\right]\left[Ferr\right] = K_1' \left[e_I^-\right]\left[Ferr\right] \tag{18}$$

where K_1' is a proportionality constant. Combining Eqs. (15) and (18):

$$r_x = K_1' \frac{k_9 \left[Ferr\right]^2}{2k_7}\left(\sqrt{1+\frac{4\Phi_I \left(1-\theta_{II}\right) R_{VIS}^{abs} k_7}{k_8 k_9 \left[PC^-\right]\left[Ferr\right]}} - 1\right) \tag{19}$$

Finally, from the third, fourth and fifth hypotheses, we arrive at the following expression for the rate of cell growth under conditions in which light is the limiting factor:

$$r_x = K_3\left(\sqrt{1+K_2 \frac{r_{VIS}^{abs}}{x}} - 1\right) \tag{20}$$

where

$$K_3 = K_1' \frac{k_9 \left[Ferr\right]^2}{2k_7} \tag{21}$$

$$K_2 = \frac{4\Phi_I \left(1-\theta_{II}\right) k_7}{k_8 k_9 \left[PC^-\right]\left[Ferr\right]} \tag{22}$$

In Eq. (20), the intracellular photon absorption rate R_{VIS}^{abs} has been related to the local volumetric rate of absorption of photons r_{VIS}^{abs} in the reactor as follows:

$$r_{VIS}^{abs}\left[\frac{photons}{time \times Volume\ of\ medium}\right] = R_{VIS}^{abs}\left[\frac{photons}{time \times Volume\ of\ biomass}\right]\frac{x\left[\frac{gr\ of\ biomass}{Volume\ of\ medium}\right]}{\rho_{cel}\left[\frac{gr\ of\ biomass}{Volume\ of\ biomass}\right]} \quad (23)$$

3.2 Modeling and Analysis of Radiant Energy field.

The local spectral volumetric rate of photon absorption $r_{\lambda}^{abs}\left(\underline{r},t\right)$, is the number of photons of wavelength between λ and $\lambda + d\lambda$, locally absorbed per unit time and unit volume of culture. From its very definition we conclude that $r_{\lambda}^{abs}\left(\underline{r},t\right)$ is the local distribution over λ of the volumetric rates of photon absorption at a time t and at any position $\underline{r}$ in the PBR. This distribution can be related to the spectral density distribution of photons $n_{\lambda}\left(\underline{r},t\right)$ through the speed of light c and the spectral absorption coefficient of radiant energy $\alpha_{\lambda}\left(t\right)$, as follows

$$r_{\lambda}^{abs}\left(\underline{r},t\right) = c\,\alpha_{\lambda}\left(t\right) n_{\lambda}\left(\underline{r},t\right) \quad (24)$$

Then, the local volumetric rate of absorption of photons $r_{VIS}^{abs}\left(\underline{r},t\right)$, considering all the photons in the visible range from 400 to 700nm is

$$r_{VIS}^{abs}\left(\underline{r},t\right) = \int_{400}^{700} r_{\lambda}^{abs}\left(\underline{r},t\right) d\lambda = c\int_{400}^{700} \alpha_{\lambda}\left(t\right) n_{\lambda}\left(\underline{r},t\right) d\lambda \quad (25)$$

In Eq. (25) $\alpha_{\lambda}\left(t\right)$ is the spectral absorption coefficient of radiant energy of the homogeneous suspension. This coefficient depends on time only indirectly through the concentration of biomass and the chlorophyll content [17]. The spectral density distribution of photons $n_{\lambda}\left(\underline{r},t\right)$ at the position $\underline{r}$ and at time t is related to the spectral distribution of radiation energy density $e_{\lambda}\left(\underline{r},t\right)$

$$e_{\lambda}\left(\underline{r},t\right) = \frac{hc}{\lambda} n_{\lambda}\left(\underline{r},t\right) \quad (26)$$

where h is Planck's constant. Moreover, the local density $n_{VIS}\left(\underline{r},t\right)$, considering all the photons with wavelength in the range 400 to 700nm, is

$$n_{VIS}\left(\underline{r},t\right)=\int_{400}^{700} n_{\lambda}\left(\underline{r},t\right)d\lambda \tag{27}$$

In Eq. (25) $\alpha_{\lambda}\left(t\right)$ is experimentally measured, and $n_{\lambda}\left(\underline{r},t\right)$ can be obtained by numerical simulation, using the methodology based on the Monte Carlo method proposed by Heinrich et al [15-18].

Light is unevenly distributed in the reactor because of the phenomena of absorption, scattering, reflection, etc, associated with the transfer of radiant energy and with the configuration of the PBR. The stratification of light increases along with algal growth, giving rise to zones with different local volumetric rate of absorption $r_{VIS}^{abs}\left(\underline{r},t\right)$ and different local volumetric density $n_{VIS}\left(\underline{r},t\right)$ of photons with wavelength in the visible region of the spectrum. The stratification of the light in the reactor is of importance to the design, scaleup, and optimization the photobioreactor.

To quantify the degree of stratification of the light in the photobioreactor, lets asume that the product $g\left(r_{VIS}^{abs},t\right)dr_{VIS}^{abs}$ is the fraction of the total culture volume with volumetric rate of photon absorption between r_{VIS}^{abs} and $r_{VIS}^{abs}+dr_{VIS}^{abs}$. The cumulative volume fraction with volumetric rate of photon absorption in the interval $\left(0,r_{VIS}^{abs}\right)$ is

$$\frac{V\left(r_{VIS}^{abs},t\right)}{V}=\int_{0}^{r_{VIS}^{abs}} g\left(\hat{r}_{VIS}^{abs},t\right)d\hat{r}_{VIS}^{abs} \tag{28}$$

where $V\left(r_{VIS}^{abs},t\right)$ is the cumulative volume of the suspension with volumetric rates of photon absorption in the interval $\left(0,r_{VIS}^{abs}\right)$ and $\hat{r}_{VIS}^{abs}$ is an integration variable running over the open interval $\left(0<\hat{r}_{VIS}^{abs}<r_{VIS}^{abs}\right)$. In particular, $V\left(r_{VIS}^{abs},t\right)$ has been assessed for every value of r_{VIS}^{abs} using the Monte Carlo method proposed by Heinrich *et al* [15-18]. Realizing the condition $\lim_{r_{VIS}^{abs}\to\infty} V\left(r_{VIS}^{abs},t\right)=V$, from Eq. (28) we can readily conclude that $g\left(r_{VIS}^{abs},t\right)$ is normalized to unity

$$\lim_{r_{VIS}^{abs}\to\infty}\frac{V\left(r_{VIS}^{abs},t\right)}{V}=\lim_{r_{VIS}^{abs}\to\infty}\int_{0}^{r_{VIS}^{abs}} g\left(\hat{r}_{VIS}^{abs},t\right)d\hat{r}_{VIS}^{abs}=1 \tag{29}$$

From Eqs. (28) and (29) we can conclude that $g\left(r_{VIS}^{abs},t\right)$ is the volume distribution function among all possible rates of photon absorption. The relationship between $\frac{V\left(r_{VIS}^{abs},t\right)}{V}$ and $g\left(r_{VIS}^{abs},t\right)$, inverse to that of Eq. (28), is

$$\frac{1}{V}\frac{dV\left(r_{VIS}^{abs},t\right)}{dr_{VIS}^{abs}} = g\left(r_{VIS}^{abs},t\right) \tag{30}$$

This, in turn, can be numerically approximated as follows

$$\frac{1}{V}\left[\frac{V\left(r_{VIS}^{abs}+\Delta r_{VIS}^{abs},t\right)-V\left(r_{VIS}^{abs},t\right)}{\Delta r_{VIS}^{abs}}\right] \approx g\left(r_{VIS}^{abs},t\right) \tag{31}$$

for sufficiently small values of Δr_{VIS}^{abs}.

In Fig. 3 one can see how the stratification of light changes along with algal growth, giving rise to zones with different local volumetric rates of absorption. When the biomass concentration is low, the reactor operates with low rates of absorption because the absorption coefficient is low in the suspension and while the concentration of photons is high. As the suspended biomass increases, the zones nearer to the lamp show higher rates of absorption, however, this high absorption will reduce the concentration of photons in the deeper zones, which will operate at slower absorption rates. These results were thoroughly discussed in a previous communication [17].

<Figure 3>

Figura 3: The distribution function $g\left(r_{VIS}^{abs},t\right)$ in terms of volumetric rates of absorption of photons for different biomass concentrations: (a) Day 6: 57.3 mg L^{-1}; (b) day 9: 135.0 mg L^{-1}; (c) day 12: 219.2 mg L^{-1}; (d) day 15: 311.7 mg L^{-1}. Corresponding to 0.34% CO_2 concentration in the air stream.

3.3 The algal growth in the PBR and regression of intrinsic kinetic parameters

In Fig. 4A, 4B and 4C the biomass growth in experiments carried out at three different concentration of carbon dioxide in the feed gas stream: 0.034 % (A- atmospheric concentration);0.34 % (B); and 3.4 %

(C). Increasing the CO_2 concentration in the gas phase brings about shifts of the acid-base equilibrium favouring the formation of carbonate group, thus lowering the pH of the culture medium. If a base is added to offset this effect, then the ionic strength and osmotic pressure of the culture is altered. Since algae growth depends on these physicochemical properties, the initial formulation of the culture medium was changed (Table I) so that the pH, the ionic strength and the osmotic pressure are equal in all the cases tested. A further modification made on the original formulation of medium BBM, consists in the use of urea as the nitrogen source instead of $NaNO_3$, in order to avoid changes of pH of the medium produced by the metabolism of NO_3^-. In this way, the pH was maintained within the range from 7.0 to 7.2 throughout the culture time in the three experiments.

<Figure 4>

Figure4: experimental values (◊) and theoretical (—) of the biomass concentration [g L^{-1}] versus time [day] for the three conditions tested CO_2. (a) 0.034%. (b) 0.34%. (c) 3.4%.

In all cell cultures the chlorophylls concentration was followed during the cultivation time (15 days).The experimental results showed that the intracellular content of total chlorophylls remained unchanged at a concentration of 2.4 mg Chl per 100 mg biomass (data not shown). As can be seen in Fig. 4, in all three cases cell growth progresses similarly although there is a big difference between the concentrations of CO_2 in the gas stream. From these results it is possible to conclude that under these lighting conditions, growth is independent of the concentration of CO_2 in the feed stream and light is the limiting substrate for growth. To take into account the ligth stratification, in this work the average cell growth rate $\overline{r}_x$ was calculated according to Eq. (32), instead of substituting a volume averaged rate of absorption of photons $\overline{r}_{VIS}^{abs}$ in Eq. (20):

$$\overline{r}_x = \int_0^{\infty} K_3 \left(\sqrt{1 + K_2 \frac{r_{VIS}^{abs}}{x}} - 1 \right) g\left(r_{VIS}^{abs}, t\right) dr_{VIS}^{abs} \qquad (32)$$

The parameter regression based on all the experimental data was performed using a genetic algorithm, with the following results: $K_3 = 4.982 \times 10^4 \left[g\, L^{-1} day^{-1} \right]$ and $K_2 = 2.541 \times 10^{-6} \left[s\, g\, \mu mol^{-1} \right]$. In Figs. 4A,

B and C, the solid line represents the growth curve as predicted with the kinetic model and for each initial biomass concentration. Predicted results show a good agreement with the observed data.

4.- CONCLUSIONS.

A kinetic expression for algal growth under light controlling conditions has been derived from a simplified pathway of the light-dependent step of photosynthesis. Such expression includes two adjustable parameters, which are clearly related to the kinetic constants and other parameters of the simplified mechanism, but above all allows for a clear identification of the local rate of photon absorption $r_{VIS}^{abs}\left(\underline{r},t\right)$ with wavelengths in the range $400<\lambda<700\ nm$, as the property of the radiation field which should integrate that expression and the mathematical way in which it should appear in the kinetics. The average cell growth rate $\overline{r}_x$ was calculated taking into account the uneven distribution of light in the reactor because of the phenomena of absorption, scattering, reflection, etc, associated with the transfer of radiant energy and with the configuration of the PBR. For this, a methodology for the simulation of the radiant field throughout the suspension is applied, which allows not only predicting the density of radiant energy at each position in the crop, but also knowing its spectral composition, and calculate the rate at which energy is locally absorbed. Based on $\overline{r}_x$, the growth of algae as a function of time was simulated, showing good agreement with experimental data for different operating conditions.

5- ACKNOWLEDGMENTS.

Funds were provided by Universidad Nacional del Litoral (CAI+D/PI: *"Análisis, síntesis, simulación y optimización de procesos biotecnológicos empleando algas microscópicas: cambio de escala racional para la producción de aceites para biodiesel y otras aplicaciones (bio)tecnológicas"*) and Consejo Nacional de Investigaciones Científicas y Técnicas de la República Argentina (CONICET) (PIP: *"Procesos biológicos empleando microorganismos fotosintéticos: desarrollo de una plataforma biotecnológica para la producción de biomasa y metabolitos derivados"*). The authors are grateful to Mr. Ramón A. Saavedra and Mr. Antonio Negro for the technical support provided.

6.- BIBLIOGRAFÍA

[1] R.B. Draaisma, R.H. Wijffels, P.M. Slegers, L.B. Brentner, A. Roy, M.J. Barbosa. Food commodities from microalgae. Curr. Opin. Biotechnol. 24:2 (2012) 169–177.

[2] R.H. Wijffels, M.J. Barbosa. An outlook on microalgal biofuels. Science. 329:5993 (2010) 796–799.

[3] M. A. Borowitzka. Culturing microalgae in outdoor ponds. In: R. A. Andersen (Ed.), Algal Culturing Techniques Elsevier, San Diego, 2005, pp. 205‑218.

[4] P.W. Behrens. Photobioreactors and fermentors: the light and dark sides of growing algae. In: R. A. Andersen (Ed.) Algal Culturing Techniques. Elsevier, San Diego. 2005, pp. 189‑204

[5] Y. Chisti. Biodiesel from microalgae. Biotechnol. Adv. 25 (2007) 294‑306.

[6] T.M. Mata, A.A. Martins, N.S. Caetano Microalgae for biodiesel production and other applications: A review. Renewable and Sustainable Energy Reviews 14:1 (2010) 217-232

[7] O. Pulz, W. Gross. Valuable products from biotechnology of microalgae, Appl Microbiol Biotechnol 65 (2004) 635-648.

[8] P. Spoalore, C. Joannis-Cassan, E. Duran, A. Isambert. Commercial Applications of Microalgae, J BiosciBioeng 101 (2006) 87-96

[9] E.C Francisco, D.B. Neves, E. Jacob-Lopes, T.T. Franco. Microalgae as feedstock for biodiesel production: Carbon dioxide sequestration, lipid production and biofuel quality. J Chem. Technol. Biotechnol. 85(2010) 395-403

[10] L. Pilon, H. Berberoglu, R. Kandilian. Radiation transfer in photobiological carbon dioxide fixation and fuel production by microalgae. 112:17 (2011) 2639–2660

[11] Q. Huang; L. Yao; T. Liu; J. Yang. Simulation of the light evolution in an annular photobioreactor for the cultivation of Porphyridium cruentum. Chemical Engineering Science 84 (2012) 718–726

[12] M.C.A.F. Rezende, C.B.B. Costa, A.C. Costa, M.R. Wolf Maciel, R. MacielFilho. Optimization of a large scale industrial reactor by genetic algorithms. Chem. Eng. Sci. 63 (2008) 330–341.

[13] G. Olivieri, P. Salatino, A. Marzocchella. Advances in photobioreactors for intensive microalgal production: Configurations, operating strategies and applications Journal of Chemical Technology and Biotechnology. 89:2 (2014) 178-195

[14] E. Lee, J. Pruvost, X. He, R. Munipalli, L. Pilon. Design tool and guidelines for outdoor photobioreactors. Chemical Engineering Science 106 (2014) 18–29

[15] J.M. Heinrich, I. Niizawa, F.A. Botta, A.R. Trombert, H.A. Irazoqui. Stratification of the Radiation Field Inside a Photobioreactor During Microalgae Growth Photochemistry and Photobiology. 89:5 (2013) 1127–1134,

[16] I. Niizawa, J.M. Heinrich, H.A. Irazoqui, Biochemical Engineering Journal. In Press, Accepted Manuscript (2014). http://dx.doi.org/10.1016/j.bej.2014.05.002

[17] J.M. Heinrich, I. Niizawa, F.A. Botta, A.R. Trombert, H.A. Irazoqui. Analysis and design of photobioreactors for microalgae production I: Method and parameters for radiation field simulation. Photochemistry and Photobiology 88:4 (2012) 938-951

[18] J.M. Heinrich, I. Niizawa, F.A. Botta, A.R. Trombert, H.A. Irazoqui (2012) Analysis and design of photobioreactors for microalgae production II: Experimental Validation of a radiation field simulator based on a Monte Carlo algorithm. Photochemistry and Photobiology 88:4 (2012) 952-960

[19] R. M. Atlas. Handbook of Media for Environmental Microbiology. Second Ed. Taylor & Francis. Boca Ratón, USA. 2005.

[20] M. K. Hein, Biological examination. In Standard Methods for the Examination of Water and Wastewater, American Public Health Association, Washington (1999) 10.26–10.27 .

[21] R.J. Ritchie. Universal chlorophyll equations for estimating chlorophylls a, b, c and d and total chlorophylls in natural assemblages of photosynthetic organisms using acetone, methanol or ethanol solvents. Photosynthetica, 46:1 (2008) 115–126.

[22] H.W. Heldt. The Calvin cycle catalyzes photosynthetic CO2 assimilation. In: H.W. Heldt (Eds), Plant Biochemistry. Elsevier. San Diego, USA. 2004, pp. 165-194

[23] H.W. Heldt. The use of energy from sunlight by photosynthesis is the basis of life on earth. In: H.W. Heldt (Ed.), Plant Biochemistry. Elsevier. San Diego, USA. 2004, pp. 45-66

[24] H.W. Heldt. Photosynthesis is an electron transport process. In: H.W. Heldt (Ed.), Plant Biochemistry. Elsevier. San Diego, USA. 2004, pp. 67-114.

Table I

Table I: Modifications of the BBM medium according to the composition of the air stream.				
Species/Property	**BBM (original)**	**Modified BBM** according to CO_2 content		
		0.034%	**0.34%**	**3.4%**
NaOH [mol L^{-1}]	0.0	$1.98\ 10^{-4}$	$7.05\ 10^{-4}$	$5.88\ 10^{-3}$
NaCl [mol L^{-1}]	$4.28\ 10^{-4}$	$2.69\ 10^{-3}$	$2.12\ 10^{-3}$	0.0
pH	6.39	7.0	7.0	7.0
$NaNO_3$ [mol L^{-1}]	$2.94\ 10^{-3}$	--	--	--
Urea [mol L^{-1}]	--	$1.47\ 10^{-3}$	$1.47\ 10^{-3}$	$1.47\ 10^{-3}$
Ionicstrength [mol L^{-1}]	$8.01\ 10^{-3}$	$8.00\ 10^{-3}$	$7.94\ 10^{-3}$	$1.10\ 10^{-2}$
Osmoticpressure [mmHg]	209.6	210.2	210.2	227.4

Table II

Table II: Reactions of the light dependent phase of the photosynthesis.

Photosystem II		
$PSII \xrightarrow{h\nu} PSII + e_{II}^{-} + h_{II}^{+}$	$r_1 = \Phi_{II}\left(\theta_{II} R_{VIS}^{abs}\right)$	(1)
$e_{II}^{-} + h_{II}^{+} \rightarrow thermal\ energy$	$r_2 = k_2\left[e_{II}^{-}\right]\left[h_{II}^{+}\right]$	(2)
$h_{II}^{+} + CE_{Mn}^{0} \rightarrow CE_{Mn}^{+}$	$r_{3.1} = k_{3.1}\left[h_{II}^{+}\right]\left[CE_{Mn}^{0}\right]$	(3.1)
$h_{II}^{+} + CE_{Mn}^{+} \rightarrow CE_{Mn}^{2+}$	$r_{3.2} = k_{3.2}\left[h_{II}^{+}\right]\left[CE_{Mn}^{+}\right]$	(3.2)
$h_{II}^{+} + CE_{Mn}^{2+} \rightarrow CE_{Mn}^{3+}$	$r_{3.3} = k_{3.3}\left[h_{II}^{+}\right]\left[CE_{Mn}^{2+}\right]$	(3.3)
$h_{II}^{+} + CE_{Mn}^{3+} \rightarrow CE_{Mn}^{4+}$	$r_{3.4} = k_{3.4}\left[h_{II}^{+}\right]\left[CE_{Mn}^{3+}\right]$	(3.4)
$CE_{Mn}^{4+} + 2H_2O \rightarrow CE_{Mn}^{0} + O_2 + 4H_{int}^{+}$	$r_{3.5} = k_{3.5}\left[CE_{Mn}^{4+}\right]$	(3.5)
$e_{II}^{-} + Q + H_2O \rightarrow QH + OH_{ext}^{-}$	$r_{4.1} = k_{4.1}\left[e_{II}^{-}\right][Q]$	(4.1)
$e_{II}^{-} + QH + H_2O \rightarrow QH_2 + OH_{ext}^{-}$	$r_{4.2} = k_{4.2}\left[e_{II}^{-}\right][QH]$	(4.2)
Cytochrome and Q-Cycle		
$QH_2 + Cit_{b_6/f} \rightarrow Q + Cit_{b_6/f}^{2-} + 2H_{int}^{+}$	$r_{5.1} = k_{5.1}\left[QH_2\right]\left[Cit_{b_6/f}\right]$	(5.1)
$Cit_{b_6/f}^{2-} + PC \rightarrow Cit_{b_6/f}^{-} + PC^{-}$	$r_{5.2} = k_{5.2}\left[Cit_{b_6/f}^{2-}\right][PC]$	(5.2)
$Cit_{b_6/f}^{-} + PC \rightarrow Cit_{b_6/f} + PC^{-}$	$r_{5.3} = k_{5.3}\left[Cit_{b_6/f}^{-}\right][PC]$	(5.3)
$Cit_{b_6/f}^{2-} + Q + 2H_2O \rightarrow Cit_{b_6/f} + QH_2 + 2OH_{ext}^{-}$	$r_{5.4} = k_{5.4}\left[Cit_{b_6/f}^{2-}\right][Q]$	(5.4)
Photosystem I		
$PSI \xrightarrow{h\nu} PSI + e_{I}^{-} + h_{I}^{+}$	$r_6 = \Phi_I\left(1-\theta_{II}\right) R_{VIS}^{abs}$	(6)
$e_{I}^{-} + h_{I}^{+} \rightarrow disipación\ térmica$	$r_7 = k_7\left[e_{I}^{+}\right]\left[h_{I}^{+}\right]$	(7)
$PC^{-} + h_{I}^{+} \rightarrow PC$	$r_8 = k_8\left[h_{I}^{+}\right]\left[PC^{-}\right]$	(8)
$e_{I}^{-} + Ferr \rightarrow Ferr^{-}$	$r_9 = k_9\left[e_{I}^{-}\right][Ferr]$	(9)

Figure
Click here to download high resolution image

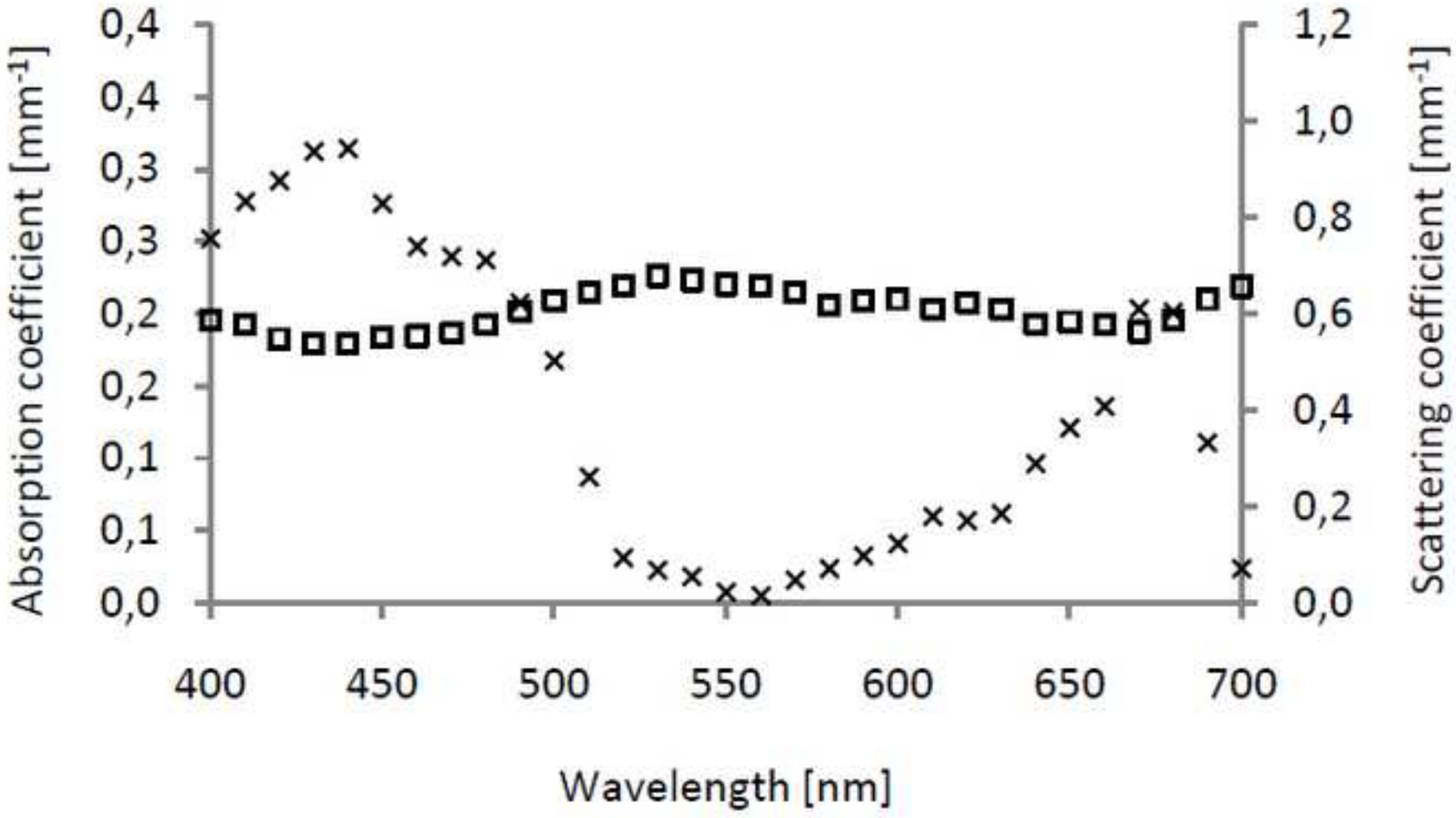

Figure 2

Click here to download high resolution image

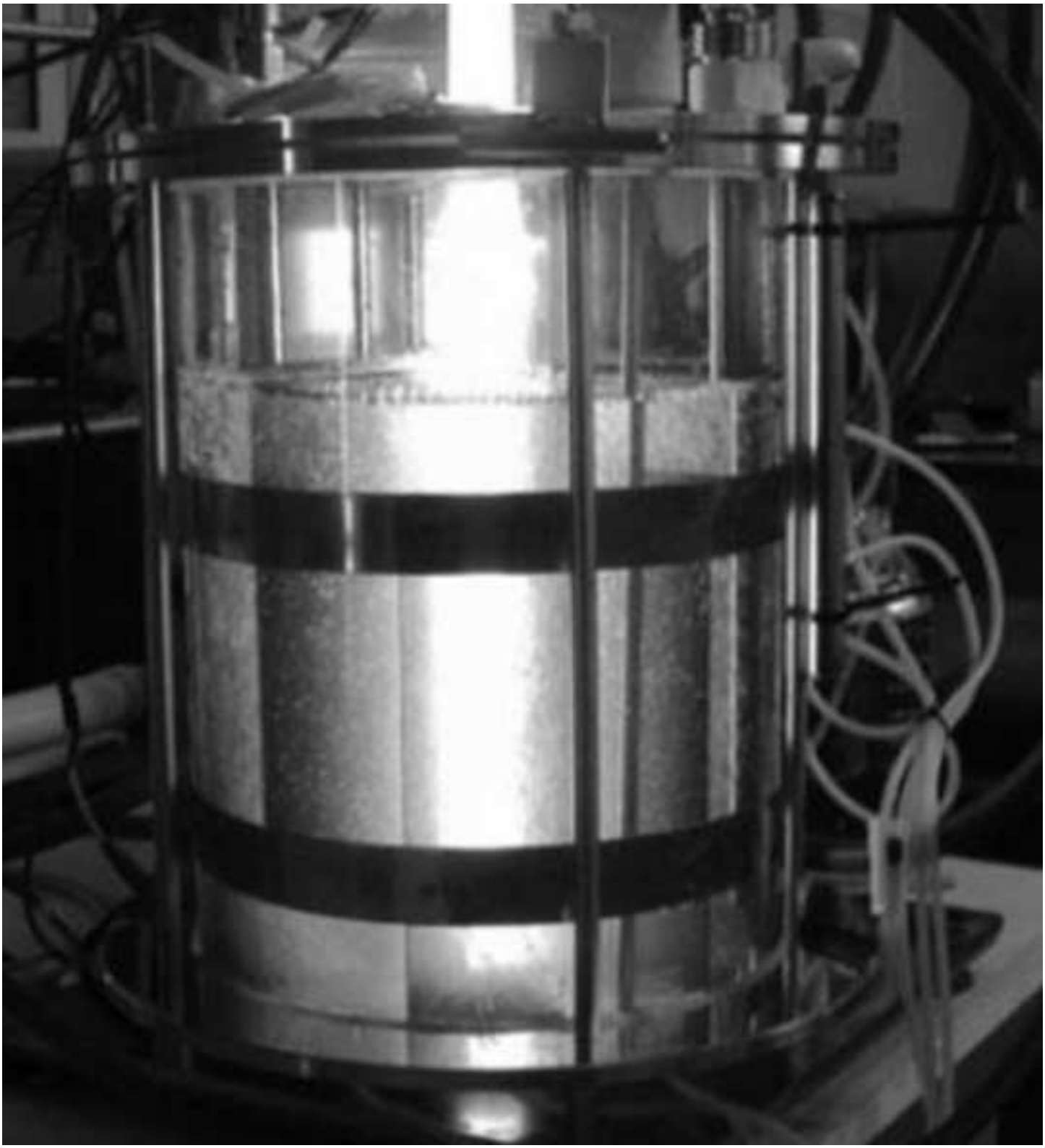

Figure 3(a)
Click here to download high resolution image

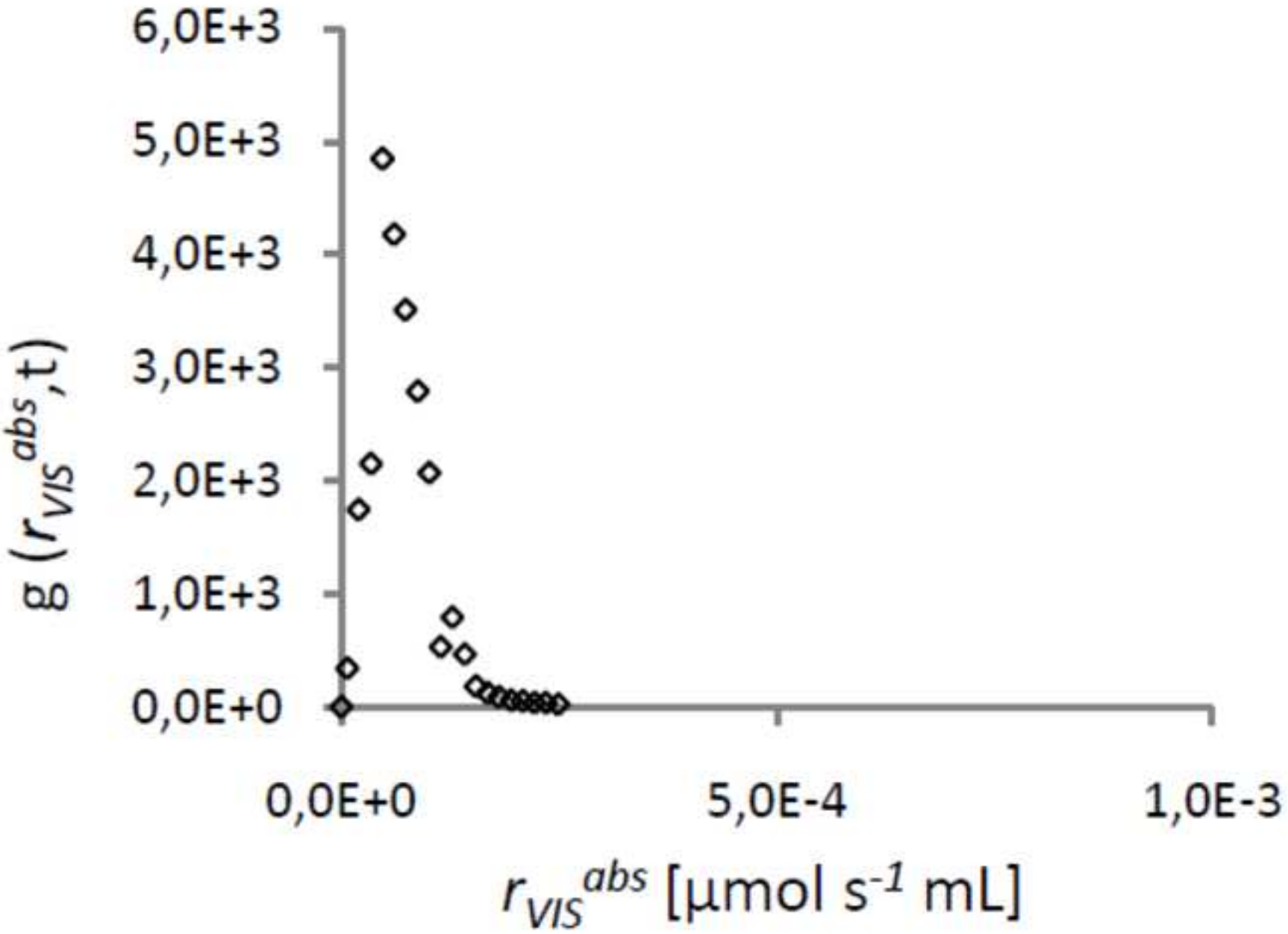

Figure 3(b)
Click here to download high resolution image

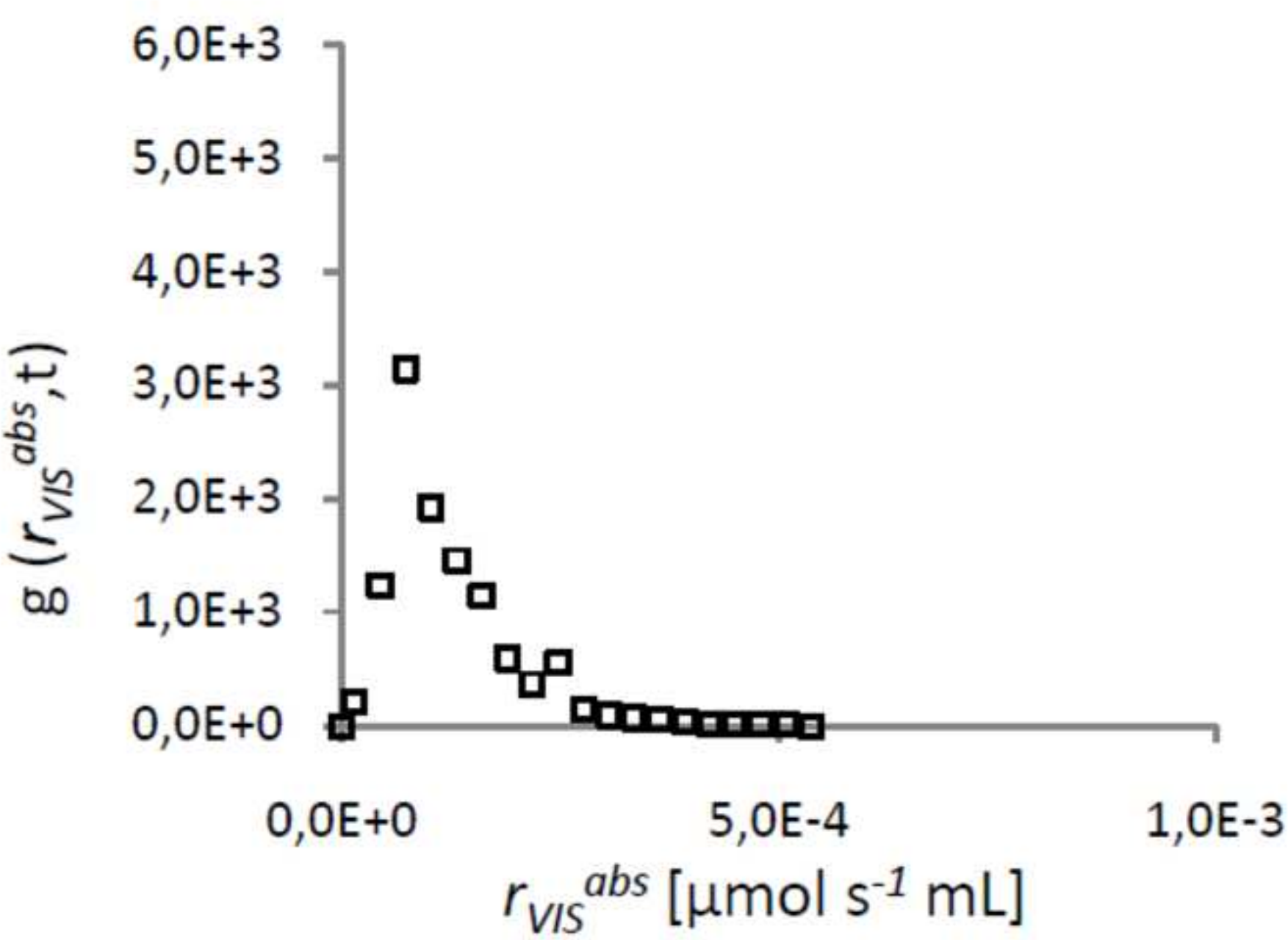

Figure 3(c)
Click here to download high resolution image

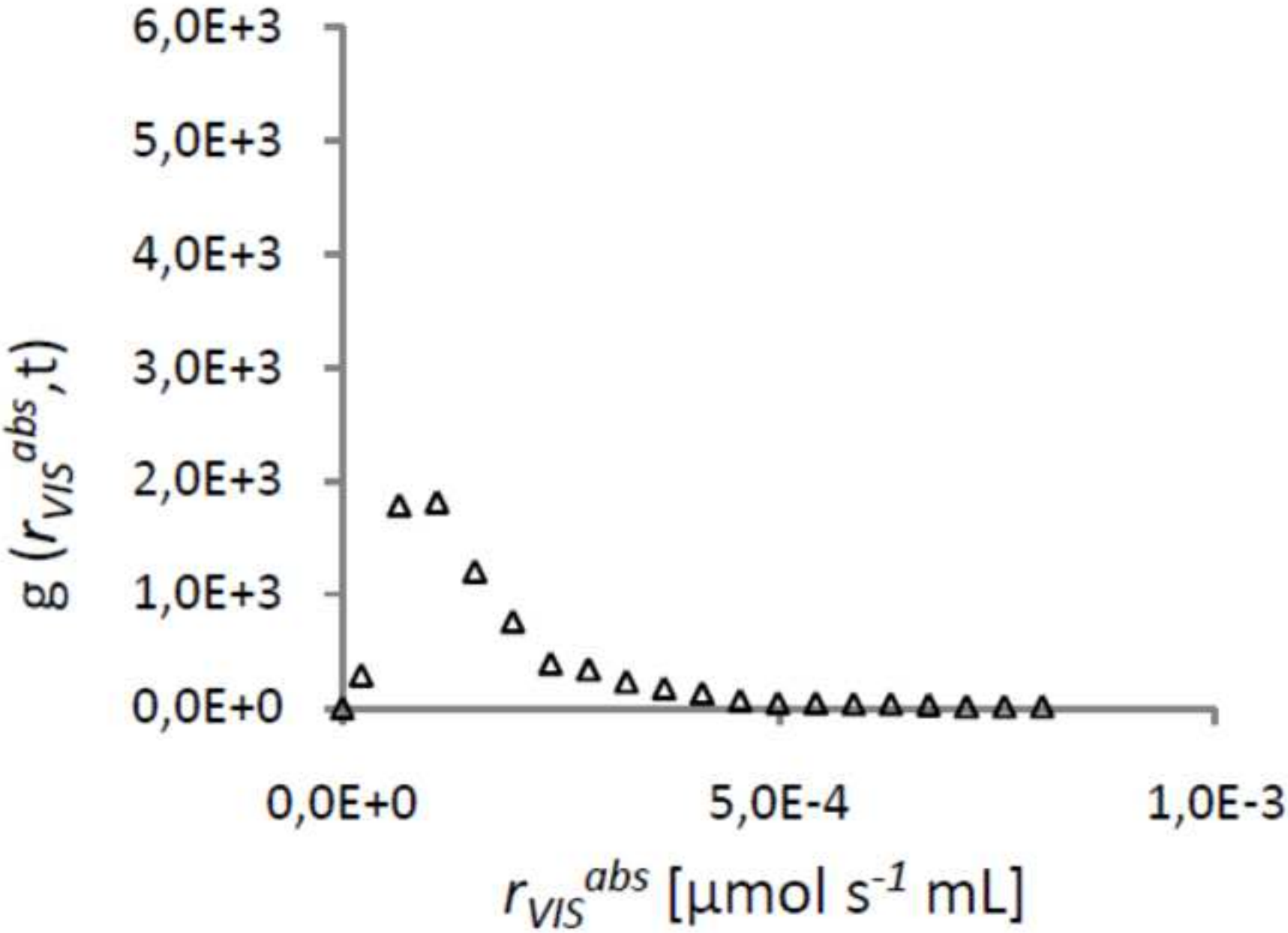

Figure 3(d)
Click here to download high resolution image

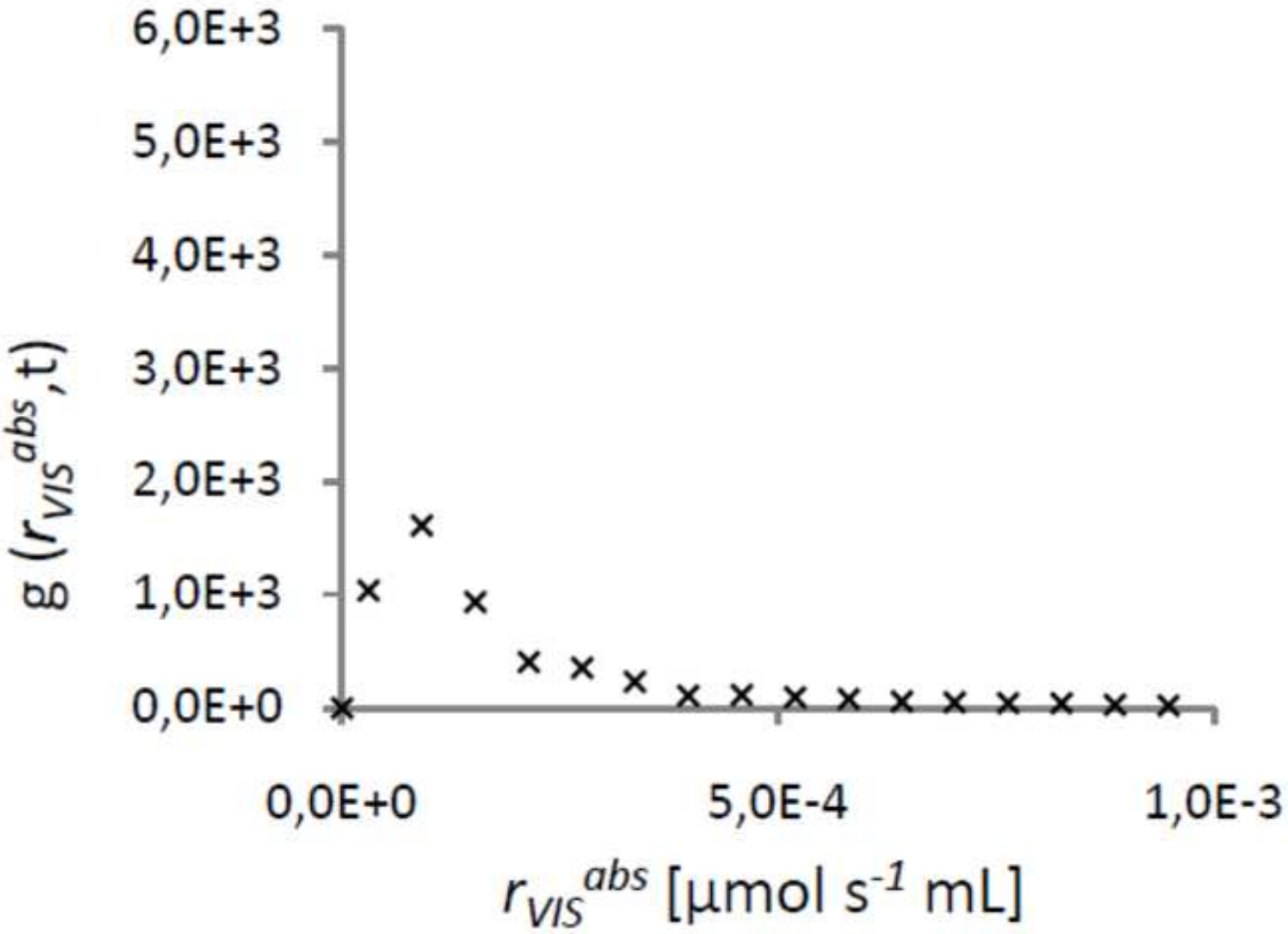

Figure 4(a)
Click here to download high resolution image

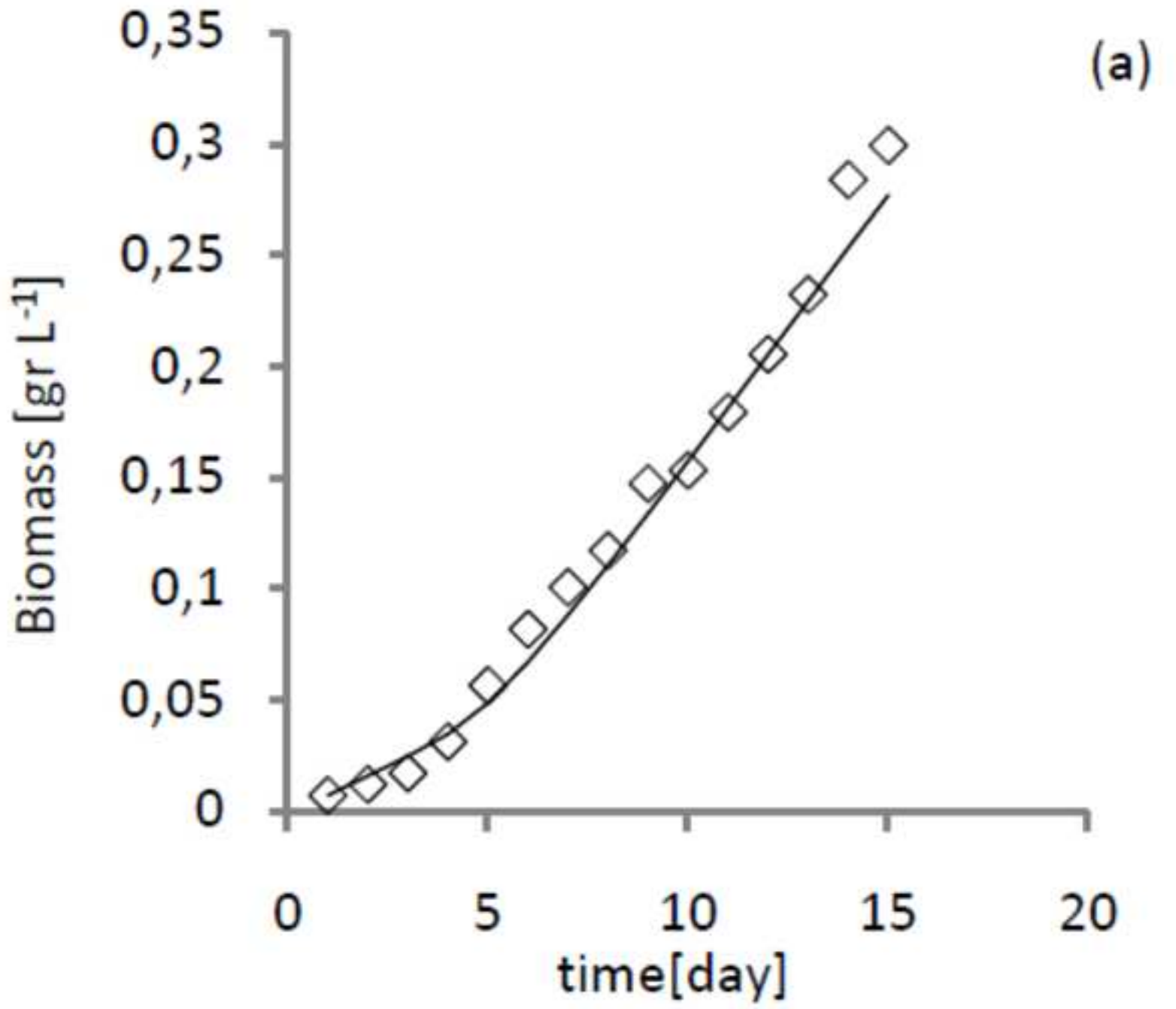

Figure 4(b)
Click here to download high resolution image

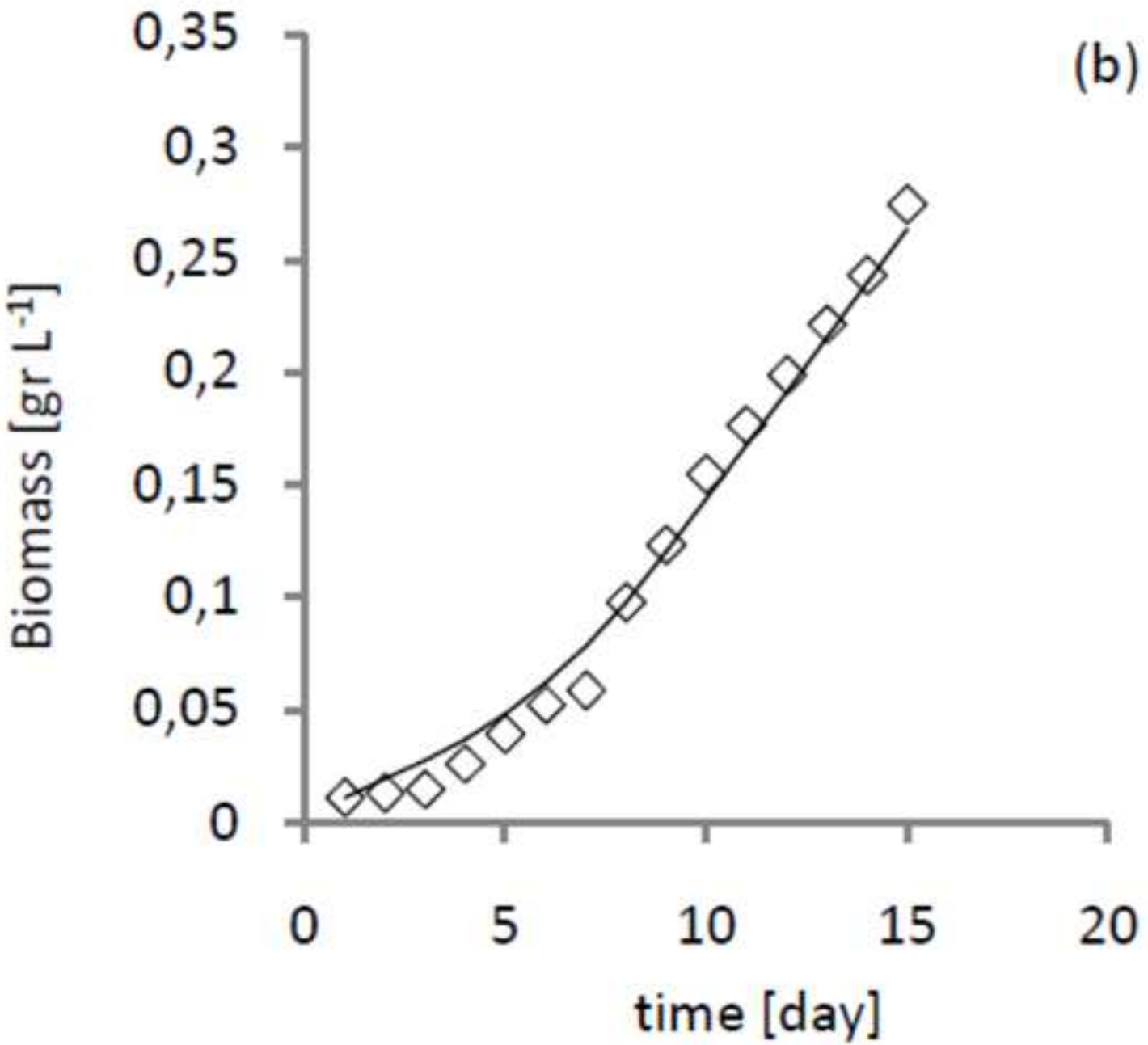

Figure 4(c)
Click here to download high resolution image